Osteoarthritis and Cartilage 26 (2018) 108–117

Osteoarthritis and Cartilage

# Angiopoietin-like protein 2 promotes chondrogenic differentiation during bone growth as a cartilage matrix factor

H. Tanoue † ‡, J. Morinaga †, T. Yoshizawa §, M. Yugami † ‡, H. Itoh † ‡, T. Nakamura ‡, Y. Uehara ‡, T. Masuda ‡, H. Odagiri ‡, T. Sugizaki †, T. Kadomatsu †, K. Miyata †, M. Endo †, K. Terada †, H. Ochi ¶, S. Takeda #, K. Yamagata §, T. Fukuda ||, H. Mizuta ‡, Y. Oike † †† *

† *Department of Molecular Genetics, Graduate School of Medical Sciences, Kumamoto University, 1-1-1 Honjo,Chuo-ku, Kumamoto 860-8556, Japan*
‡ *Department of Orthopaedic Surgery, Graduate School of Medical Sciences, Kumamoto University, 1-1-1 Honjo,Chuo-ku, Kumamoto 860-8556, Japan*
§ *Department of Medical Biochemistry, Graduate School of Medical Sciences, Kumamoto University, 1-1-1 Honjo,Chuo-ku, Kumamoto 860-8556, Japan*
|| *Department of Anatomy and Neurobiology, Graduate School of Medical Sciences, Kumamoto University, 1-1-1 Honjo,Chuo-ku, Kumamoto 860-8556, Japan*
¶ *Department of Physiology and Cell Biology, Graduate School of Medical and Dental Sciences, Tokyo Medical and Dental University, 1-5-45 Yushima, Bunkyo-ku, Tokyo 113-8510, Japan*
# *Endocrine Center, Toranomon Hospital, 2-2-2 Toranomon, Minato-ku, Tokyo, 05-8470, Japan*
†† *Core Research for Evolutional Science and Technology (CREST), Japan Agency for Medical Research and Development (AMED), Tokyo, Japan*

ARTICLE INFO

*Article history:*
Received 21 February 2017
Accepted 10 October 2017

*Keywords:*
Epiphyseal cartilage
ANGPTL2
Extracellular matrix
Differentiation
Endochondral ossification

SUMMARY

*Objective:* Chondrocyte differentiation is crucial for long bone growth. Many cartilage extracellular matrix (ECM) proteins reportedly contribute to chondrocyte differentiation, indicating that mechanisms underlying chondrocyte differentiation are likely more complex than previously appreciated. Angiopoietin-like protein 2 (ANGPTL2) is a secreted factor normally abundantly produced in mesenchymal lineage cells such as adipocytes and fibroblasts, but its loss contributes to the pathogenesis of lifestyle- or aging-related diseases. However, the function of ANGPTL2 in chondrocytes, which are also differentiated from mesenchymal stem cells, remains unclear. Here, we investigate whether ANGPTL2 is expressed in or functions in chondrocytes.

*Methods:* First, we evaluated *Angptl2* expression during chondrocyte differentiation using chondrogenic ATDC5 cells and wild-type epiphyseal cartilage of newborn mice. We next assessed ANGPTL2 function in chondrogenic differentiation and associated signaling using *Angptl2* knockdown ATDC5 cells and *Angptl2* knockout mice.

*Results:* ANGPTL2 is expressed in chondrocytes, particularly those located in resting and proliferative zones, and accumulates in ECM surrounding chondrocytes. Interestingly, long bone growth was retarded in *Angptl2* knockout mice from neonatal to adult stages via attenuation of chondrocyte differentiation. Both *in vivo* and *in vitro* experiments show that changes in ANGPTL2 expression can also alter p38 mitogen-activated protein kinase (MAPK) activity mediated by integrin α5β1.

*Conclusion:* ANGPTL2 contributes to chondrocyte differentiation and subsequent endochondral ossification through α5β1 integrin and p38 MAPK signaling during bone growth. Our findings provide insight into molecular mechanisms governing communication between chondrocytes and surrounding ECM components in bone growth activities.



## Introduction

Endochondral ossification is critical to production of sufficient bone matrix during bone development and body growth[1]. For physiological ossification to occur, chondrogenic cells must first undergo differentiation[1]. Initially, undifferentiated mesenchymal

* Address correspondence and reprint requests to: Y. Oike, Department of Molecular Genetics, Graduate School of Medical Sciences, Kumamoto University, 1-1-1 Honjo, Chuo-ku, Kumamoto 860-8556, Japan. Fax: 81-96-373-5145.
*E-mail address:* oike@gpo.kumamoto-u.ac.jp (Y. Oike).

https://doi.org/10.1016/j.joca.2017.10.011
1063-4584/

stem cells condense and become immature chondrocytes, which then undergo differentiation to become hypertrophic chondrocytes that serve as master regulatory cells of bone matrix production[1]. Cartilage is an organ composed only of chondrocytes and surrounding extracellular matrix (ECM) without vessels or lymph ducts[2]. Cartilage ECM controls chondrocyte ECM activity by delivering nutrients, supporting metabolism and physically protecting cells[3,4]. Furthermore, cartilage functions to maintain chondrocyte homeostasis in activities such as differentiation or endochondral ossification via signaling from cartilage components such as collagen fibers and fibronectin[5,6]. Also, in endochondral ossification, steps related to chondrocyte differentiation are controlled by extracellular signaling cascades such as mitogen-activated protein kinase (MAPK)-related pathways regulated by various ECM factors[5,7,8]. Particularly, p38 MAPK pathways are reportedly a major signaling pathway controlling chondrocyte maturation, hypertrophy and endochondral ossification[7,9,10].

Angiopoietin-like protein (ANGPTL) 2, a secreted signaling factor that exhibits N-terminal coiled-coil and C-terminal fibrinogen-like domains, is abundantly expressed in adipocytes and ligament fibroblasts, both of which differentiate from mesenchymal stem cells[11–13]. Previous reports suggest that ANGPTL2 activates several intracellular signaling factors, including MAPKs, in the progression of several diseases[14,15]. Although chondrocytes are part of the mesenchymal stem cell lineage, expression and potential function of ANGPTL2 in chondrocytes have not yet been clarified[11].

Here, we evaluated ANGPTL2 expression and function in chondrocyte differentiation and subsequent endochondral ossification using the mouse chondrogenic line ATDC5[16]. We also asked whether ANGPTL2 is expressed in chondrocytes during bone development and wound repair following fracture in wild-type mice. We also observed that long bone growth in *Angptl2* knockout mice was slower than that seen in wild-type mice. This is the first report showing that ANGPTL2 functions as an ECM matrix protein in chondrocyte differentiation and subsequent endochondral ossification.

## Materials and methods

### *Mice*

All procedures were in accordance with guidelines for care and use of laboratory animals approved by the Kumamoto University Ethics Review Committee for Animal Experimentation. Animals were bred in a mouse house with automatically controlled lightening (12 h on, 12 h off), and a stable temperature of 23°C was maintained throughout the study. *Angptl2*-knockout and wild-type littermate mice on a C57BL/6N background were used for all animal experiments, as described[12].

### *ATDC5 cell culture*

The murine chondrogenic line ATDC5 was purchased from the Riken BioResource Center (Ibaraki, Japan). Cells were cultured in Dulbecco's Modified Eagle's Medium/Nutrient F-12 Ham (DMEM/F12) (Sigma–Aldrich, St Louis, MO) containing 5% FCS, 1% penicillin/streptomycin (Thermo Fisher Scientific, Waltham, MA), 10 μg/ml human transferrin (Sigma–Aldrich), $3 \times 10^{-8}$ M sodium selenite (Sigma–Aldrich), and 37.5 μg/ml ascorbate 2-phosphate (Wako, Osaka, Japan), as described[16–18]. Cells were maintained at 37°C in a humidified atmosphere of 5% $CO_2$ in air for the entire culture period. To induce chondrogenic differentiation, 10 μg/ml human insulin (Sigma–Aldrich) was added to the medium and supplemented to cultures when medium was changed.

### *Real-time polymerase chain reaction (PCR) analysis*

RNA was extracted from ATDC5 cells or from epiphyseal cartilage of newborn mice using TRIzol reagent (Invitrogen, Carlsbad, CA). After reverse transcription of RNA using a PrimeScript RT Reagent Kit (Takara Bio, Shiga, Japan), real-time PCR analyses were performed using SYBR Premix Ex Taq II (Takara Bio) and a Thermal Cycler Dice Real Time system (Takara Bio), as described[12]. Primer sequences are shown in Table S1.

### *Angptl2 knockdown in ATDC5 cells*

For *Angptl2* knockdown, oligonucleotides representing *Angptl2* small hairpin (sh) RNA (target sequence: 5′-CCAGAAAGC GAGTACTATA-3′) were cloned and ligated into the pSIREN-RetroQ (Clontech Lab., Inc., Mountain View, CA) expression vector. After transfection of the retroviral packaging line Plat-E cells with sh or pSIREN-RetroQ-control vector, retrovirus-containing medium was mixed with polybrene and added to ATDC5 cells for infection. Cells were selected in puromycin (5 μg/ml)[19,20].

### *Angptl2 or Itgb1 knockdown in ATDC5 cells*

*Angptl2 or Itgb1* knockdown in ATDC5 cells was performed using siRNA (Thermo Fisher Scientific) according to the manufacturer's instruction. Lipofectamine RNAiMAX (Thermo Fisher Scientific) was used for siRNA transfection.

### *Treatment of ATDC5 cells with recombinant ANGPTL2*

ATDC5 cells were maintained 24 h in DMEM/F12 containing 0% FCS. Cells were then treated with recombinant ANGPTL2 protein (5 μg/ml) prepared as described[15].

### *Treatment with integrin α5β1 antibody or p38 MAPK inhibitor*

ATDC5 cells were pretreated with anti-α5β1 integrin antibody (25 mg/ml) (Merck Millipore, Darmstadt, Germany), 10 nM SB-203580 (p38 MAPK inhibitor, Wako) or both for 1 h before recombinant ANGPTL2 treatment. 25 mg/ml Rat IgG (Merck Millipore) served as a control for the anti-α5β1 integrin antibody, and methanol served as vehicle control for SB-203580.

### *Histology*

Bone samples were obtained from newborn or 12–14 week-old mice. Bone fixation was performed according to standard protocols[21]. Briefly, mouse hindlimbs were fixed in 10% formalin overnight and then decalcified in 10% EDTA (pH 7.4) at room temperature for 3 days with shaking (demineralization was performed in specimens older than P7). After paraffin-embedding, longitudinal serial sections (4 μm) of tibiae and femurs were collected. After deparaffinisation, hematoxylin and eosin (H&E) or toluidine blue staining (for cartilage) was performed using a standard protocol as described[22]. In newborn mice, distal epiphyseal cartilage of the femur was cut for quantification after mice were euthanized. Histological analysis of the longitudinal length of hypertrophic zones was conducted by observers blinded to mouse genotypes, based on procedures reported by Tian *et al.*[23] using ImageJ software (National Institutes of Health (NIH), Bethesda, MD).

### *Immunohistochemistry*

Dissected mouse limbs embedded in paraffin were cut (4 μm) and air-dried, and sections were deparaffinized. For Indian

hedgehog (IHH), COLLAGEN II, ACAN, and COLLAGEN X immunostaining, antigen retrieval was performed by a 30-min incubation in hyaluronidase (25 mg/ml in PBS) (Sigma–Aldrich). For ANGPTL2 immunostaining, sections were heated to 95°C for 1 h in Target Retrieval Solution (Dako, Glostrup, Denmark) before hyaluronidase treatment. For SOX9 and Ki-67 immunostaining, tissue sections were heated to 60°C overnight in Target Retrieval Solution (Dako) for antigen retrieval. Sections were pretreated in 3% $H_2O_2$ in PBS to inhibit endogenous peroxidases. Slides were blocked with Block-Ace Powder (4 g/100 ml in PBS) (DS PHARMA BIOMEDICAL, Osaka, Japan) for 1 h. Specimens were incubated overnight at 4°C with antibody against rabbit anti-mouse IHH polyclonal antibody (1:300) (ab-39634, Abcam Cambridge, UK), rabbit anti-bovine COLLAGEN II polyclonal antibody (1:100) (LB-1297; LSL Biolafitte, St. Germain-en-Laye, France), rabbit anti-human ACAN polyclonal antibody (1:200) (GTX113122; GeneTex, Irvine, CA), rabbit anti-rat COLLAGEN X polyclonal antibody (1:300) (LB-0092; LSL Biolafitte), rabbit anti-mouse ANGPTL2 monoclonal antibody (2E3, 25 μg/ml)[24], Ki-67 (1:600) (#NCL-Ki-67p; Leica, Wetzlar, Germany), or rabbit anti-mouse SOX9 polyclonal antibody (1:500) (AB5535; Millipore). Normal rabbit IgG Tris-buffered saline (sc-2027; Santa Cruz Biotechnology, Santa Cruz, CA) served as negative control. For ANGPTL2 and IHH, staining was performed using a Tyramide Signal Amplification (TSA) kit (Perkin Elmer, Boston, MA). For COLLAGEN X, COLLAGEN II, ACAN, Ki-67, and SOX9, samples were treated with goat anti-rabbit Ig [F(ab')2] conjugated with peroxidase (Dako) as secondary antibody, based on the manufacturer's protocol. Peroxidase activity was visualized by incubation with a 3, 3-diaminobenzidine solution followed by fast green counterstaining.

*Immunoelectron microscopy*

Paraffin sections were immunostained for ANGPTL2 as above, postfixed with 1% $OsO_4$, stained en bloc with uranyl acetate, and embedded in epoxy resin. Resin blocks were detached from slides as before[25], and ultrastructures were observed in an electron microscope (H-7700, Hitachi, Tokyo, Japan).

*Immunoblot analysis*

Immunoblot analysis was performed as described[26]. In brief, Super Sep Ace gels (5–20%) were from Wako. Antibodies were against phospho-ERK1/2 and ERK1/2, phospho-JNK and JNK, phospho-p38 and p38 (Cell Signaling Technology, Danvers, MA), HSC70 (B-6, Santa Cruz Biotechnology), Integrin β1 (ab-179471, Abcam) and ANGPTL2 (R&D Systems, Minneapolis, MN). Immunodetection was performed using an enhanced chemiluminescence (ECL) kit (GE Healthcare, Amersham, UK).

*Laser microdissection of neonatal epiphyseal cartilage sections*

Microdissection was performed using a LMD 7000 system (Leica), according to the manufacturer's instructions. In brief, paraffin-embedded hindlimbs from neonatal mice were cut into 20 μm-thick sections and mounted on Membrane Slides (Leica). After staining slides with toluidine blue, growth plate zones were microscopically dissected and collected from samples ($n = 6$ mice). Cartilage was divided into resting (Re), proliferative (Pr), or hypertrophic (Hy) zones [Fig. 2(A)].

*Droplet digital PCR*

RNA was isolated from microdissected epiphyseal cartilage using RNeasy FFPE kit (Qiagen, Venlo, Netherlands). After reverse transcription using PrimeScript RT master mix (TaKaRa), droplet digital PCR (ddPCR) for *Angptl2*, *Itga5*, *Itgb1*, *Pirb*, and *Rps18* transcripts was carried out using a QX200 ddPCR system (Bio-Rad Laboratories, Hercules, CA), according to the manufacturer's instruction. Data was analyzed using QuantaSoft analysis software (Bio-Rad), and transcripts were quantified as copies/μl of PCR reaction. *Angptl2*, *Itga5*, *Itgb1*, and *Pirb*, transcript levels were normalized to *Rps18* levels.

*Alcian blue and Alizarin red staining of long bones*

Skeletons of newborn mice were fixed in 95% ethanol overnight and stained with Alcian blue and Alizarin red, according to standard protocols[23]. Femurs and tibiae were photographed with a ruler, and ossified bone length was measured using ImageJ software (NIH).

*Limb length measurement*

Femurs and tibiae were photographed with a ruler, and bone length was measured using ImageJ software (NIH).

*Statistical analysis*

All data are presented as means ± 95 percent confident interval (CI). Comparisons between two groups were made using Student's *t* test or Welch's *t* test. To compare three or more groups, the Kruskal–Wallis test was used. Statistical analysis was performed using GraphPad PRIZM software (GraphPad Software, Inc., La Jolla, CA). $P < 0.05$ was considered statistically significant.

## Results

*Angptl2 is expressed at an early phase of chondrocyte differentiation*

First, we evaluated expression patterns of ANGPTL2 in comparison with chondrocyte differentiation markers *in vitro* using the mouse chondrogenic line ATDC5, which undergo differentiation in the presence of insulin[15]. Seven days after the start of insulin treatment (day 0), expression of the proliferative chondrocyte marker *Col2a1* and *Aggrecan* (*Acan*) peaked [Fig. 1(A), left and middle]. By contrast, expression of the hypertrophic chondral marker *Col10a1* was detected at day 14 and 21 after differentiation [Fig. 1(A) right]. By day 21 of differentiation, cells also showed increased alkaline phosphatase (ALP) activity [Fig. S1(A)], suggesting that they were becoming hypertrophic. Interestingly, among *Angptl* family members 1–8, transcript levels of *Angptl2* were highest, while *Angptl1*, *6* and 7 weren't detected on any day of the differentiation period [Fig. S1(B)]. Furthermore, *Angptl2* transcript levels were relative high at early phases of ATDC5 differentiation, peaking at day 7, but then significantly decreased by the hypertrophic chondral phase (day 21) [Figs. 1(B), S1(B)].

*Angptl2 knockdown suppresses chondrocyte differentiation*

We next asked whether *Angptl2* knockdown altered chondrocyte differentiation. To do so, we prepared ATDC5 cells in which *Angptl2* expression was stably silenced by small hairpin (sh) RNA [Fig. 1(C)]. Then, these cells were induced to differentiate into hypertrophic chondrocyte by insulin treatment. On day 7 of differentiation, a point when expression of the proliferating chondrocyte marker *Col2a1* and *Acan* was increasing [Fig. 1(A)], real-time PCR analysis revealed no significant change in *Col2a1* and *Acan* expression in *Angptl2* knockdown relative to control shRNA control cells [Fig. 1(D)]. At differentiation day 21, when expression of the hypertrophic chondrocyte marker *Col10a1* normally increased [Fig. 1(A)], real-time PCR analysis revealed significantly decreased

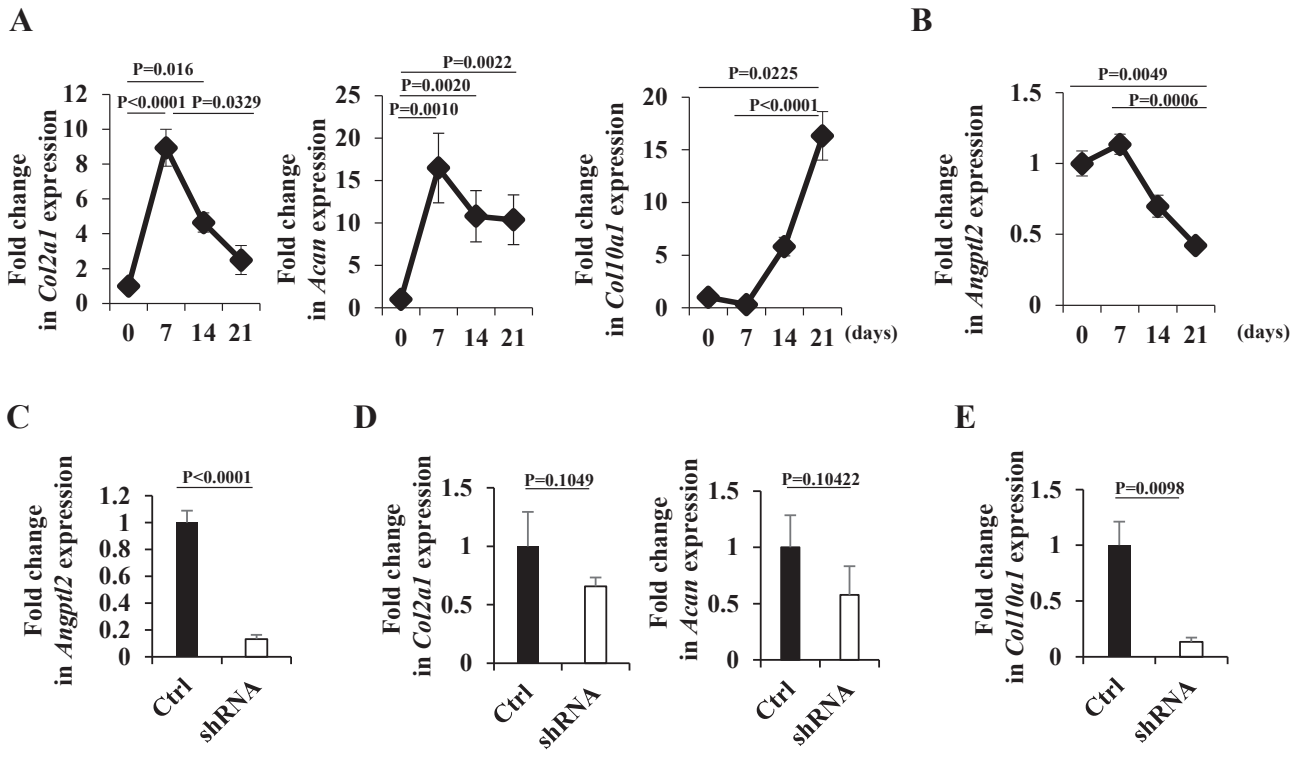


**Fig. 1. Resting and proliferative chondrocytes express *Angptl2 in vitro* and *Angptl2* knockdown suppresses chondrocyte differentiation**. (A) Graphs showing mRNA expression of *Col2a1* (left), *Acan* (middle), and *Col10a1* (right) and (B) *Angptl2* mRNA expression during chondrogenic differentiation of ATDC5 cells. Transcript levels were normalized to *18s* ribosomal RNA and expressed as fold-increases relative to day 0 ($n = 6$). (C) *Angptl2* transcript levels in ATDC5 cells stably expressing control vector (Ctrl) or *Angptl2* shRNA (shRNA). Values in control samples were set to 1 ($n = 4$). (D) *Col2a1* (left) and *Acan* (right) transcript levels on day 7 of differentiation ($n = 4$). Values are normalized to *18s* ribosomal RNA and expressed as fold increase relative to control vector. (E) *Col0a1* transcript levels on day 21 of differentiation ($n = 4$). Values are normalized as above. Results are expressed as means ± 95%CI (A, B, C, D, E).

*Col10a1* expression in *Angptl2* knockdown relative to control shRNA cells [Fig. 1(E)]. In addition, transcript levels of hypertrophic chondral markers, such as *ALP*, *Osteopontin* (*Opn*), or *Matrix metalloproteinase* (*Mmp*) *13*, as well as ALP activity, were also decreased in knockdown relative to control shRNA cells at differentiation day 21 [Fig. S1(C), (D)].

### *ANGPTL2 is expressed in resting and proliferative chondrocytes and to a lesser extent in hypertrophic chondrocytes during endochondral bone formation*

Next, we asked whether ANGPTL2 is expressed in epiphyseal cartilage and, if so, whether its expression changes as chondrocytes differentiate. To do so, we extracted RNA from wild-type distal epiphyseal cartilage from femur of neonatal mice using microdissection and estimated *Angptl2* expression levels in resting, proliferative, and hypertrophic zones [Fig. 2(A)]. Digital PCR analysis revealed significant *Angptl2* expression in both resting and proliferative zones, but little *Angptl2* expression in the hypertrophic zone [Fig. 2(B)]. Immunohistochemistry detected ANGPTL2 protein in the cytoplasm of resting and proliferating chondrocytes but not in hypertrophic chondrocytes [Figs. 2(C), S2(A)]. Interestingly, we observed ANGPTL2 accumulation in the ECM of epiphyseal cartilage [Fig. 2(C), S2(A)]. Electron microscopy analysis revealed ANGPTL2 accumulation in the ECM of epiphyseal cartilage of newborn mice (Fig. 3). Moreover, immunostaining of cultured ATDC5 cells revealed intracellular ANGPTL2 staining in undifferentiated cells and ANGPTL2 accumulation in ECM after differentiation [Fig. S2(B)]. These findings suggest that ANGPTL2 produced at early phases of chondrocyte differentiation may act as an ECM protein in cartilage differentiation.

### *Angptl2 knockout mice show impaired differentiation of immature hypertrophic chondrocytes*

To assess ANGPTL2 function in differentiation of epiphyseal cartilage, we performed histological analysis of that tissue derived from newborn *Angptl2* knockout and control mice. Both hematoxylin/eosin and toluidine blue staining of cartilage sections revealed hypertrophic chondrocytes arranged in an orderly manner in wild-type mice, whereas that arrangement was perturbed in *Angptl2* knockout mice. Moreover, we observed a decrease in the size of hypertrophic chondrocytes accompanied by an increase in the space between cells in the *Angptl2* knockout, as manifested by a thinning of the layer of hypertrophic chondrocytes relative to that seen in control wild-type littermates [Fig. 4(A–C)]. Furthermore, immunohistochemistry to detect IHH, a marker of prehypertrophic chondrocytes, and COLLAGEN X, a marker of hypertrophic chondrocytes, revealed significantly decreased protein accumulation in prehypertrophic and hypertrophic chondrocyte layers of *Angptl2* knockout compared to wild-type mice [Fig. 4(D)]. In addition, transcript levels of hypertrophic chondrocyte markers *Opn* and *Mmp13* in epiphyseal cartilage of *Angptl2* knockout neonates were lower than those in wild-type controls [Fig. S3(A)]. By contrast, we observed no change in expression or distribution of COLLAGEN II or ACAN, both of which are found in the chondrocyte ECM, between genotypes [Fig. S3(A), (B)]. These data suggest that chondrocyte

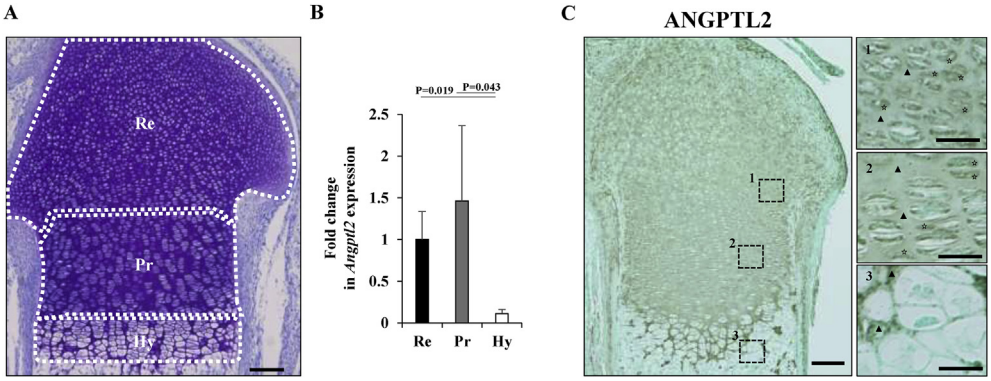


**Fig. 2. ANGPTL2 is expressed from resting and proliferative chondrocytes and accumulates in cartilage matrix**. (A) Representative image of toluidine blue staining of epiphyseal cartilage from a wild-type neonatal mouse. Re: resting zone. Pr: proliferative zone. Hy: hypertrophic zone. Scale bars = 100 μm (B) *Angptl2* transcript levels in Re, Pr, and Hy from wild-type mouse neonates. Transcription levels were normalized to *18s* ribosomal RNA and expressed as fold-increase relative to Re ($n = 4$). (C) Left panel: ANGPTL2 immunostaining in epiphyseal cartilage of a wild-type mouse. Right panels 1–3: higher magnification images of dashed squares (1–3) in left panels. Panel 1, Re; Panel 2, Pr; and Panel 3, Hy. Scale bars (left Panel) = 100 μm. Scale bars (right panels 1, 2, and 3) = 25 μm. Stars indicate ANGPTL2-positive cytoplasm. Arrowheads indicate ANGPTL2 accumulation in ECM. Results are expressed as means ± 95%CI (B).

differentiation in *Angptl2* knockout mice is incomplete relative to wild-type controls.

Next, we conducted *Angptl2* loss of function experiments in ATDC5 cells or knockout mice to investigate potential changes in chondrocyte proliferation or apoptosis. To do so, we first knocked down *Angptl2* in ATDC5 cells with small interfering (si) RNA and found significantly decreased cell proliferation in knockdown relative to control cells [Fig. S4(A), (B)]. We then stained the proliferating zone of neonatal epiphyseal cartilage of *Angptl2* knockout mice with the proliferation marker Ki-67 and found significantly decreased Ki-67 expression in knockout relative to wild-type mice, indicative of decreased chondrocyte growth [Fig. S4(C), (D)]. By contrast, analysis of apoptosis in chondrocytes of the growth plate using TUNEL staining revealed increased apoptosis in the hypertrophic zone in 12-week-old *Angptl2* knockout relative to comparable wild-type mice [Fig. S5(A), (B)]. These findings suggest that both proliferation and apoptosis of chondrocytes are altered by ANGPTL2 loss during endochondral ossification.

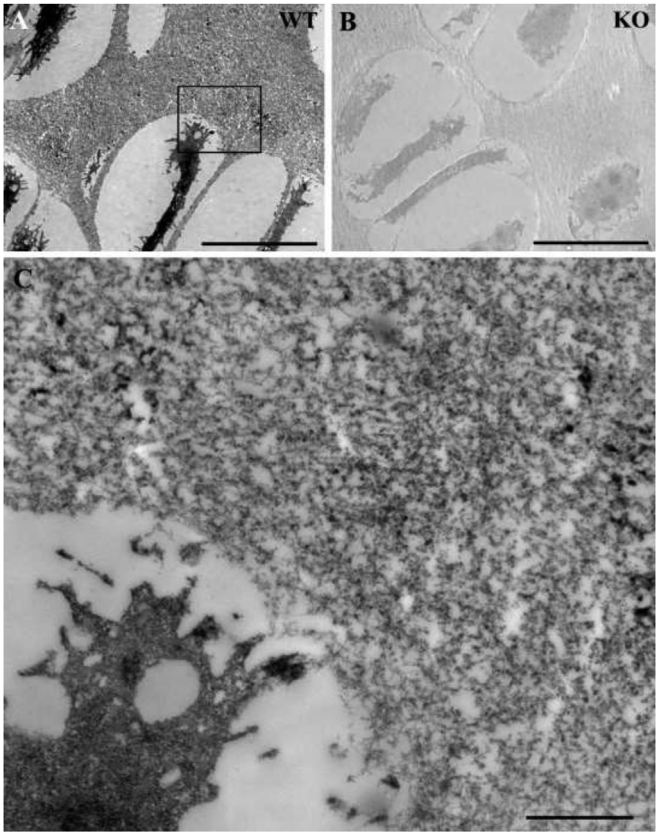


**Fig. 3. Electron micrographs showing immunoreactivity for ANGPTL2 in cartilage of newborn animals**. Tissues were taken from femur of wild type (A, C) and *Angptl2* knockout (B) mice and processed simultaneously under the same experimental conditions. Framed area in (A) is enlarged in (C). Extracellular localization of reaction products in wild type tissue is clearly observable in the cartilage matrix where both fibrous and globular materials are labeled. Chondrocyte also contains reaction products. Note lack of labeling in knockout animal as negative control (B). WT, wild-type mice; KO, *Angptl2* knockout mice. Scale bars (A, B) = 10 μm. Scale bars (C) = 1 μm.

### *ANGPTL2 activates α5β1 Integrin/p38 MAPK signaling during chondrocyte differentiation*

To assess underlying mechanisms, we performed western blotting to compare MAPK phosphorylation in epiphyseal cartilage of newborn *Angptl2* knockout and control mice, as MAPKs are critical signals for chondrocyte differentiation[7]. Interestingly, p38 MAPK phosphorylation levels markedly decreased in epiphyseal cartilage of *Angptl2* knockout mice relative to that seen in wild-type mice. On the other hand, ERK1/2 kinase phosphorylation levels were comparable in both genotypes [Fig. 5(A), (B)], and significant expression of c-jun N-terminal kinases or their phosphorylation was not observed in epiphyseal cartilage of wild-type or *Angptl2* knockout mice [Fig. 5(A)]. Both α5β1 Integrin receptor and paired Ig-like receptor B (PIRB) reportedly function as ANGPTL2 receptors in contexts other than chondrocytes[11]. Therefore, we asked which receptors functions as an ANGPTL2 receptor in chondrocytes. To do so, we first examined expression of *Itga5*, *Itgb1*, and *Pirb* in differentiated ATDC5 chondrocytes. Transcript levels of *Itga5* and *Itgb1* were high and fairly uniform in ATDC5 cells over the entire period of *in vitro* chondrocyte differentiation [Fig. 6(A)]. We also observed minimal expression of *Pirb* transcripts in ATDC5 cells at any stage of differentiation [Fig. 6(A)]. Accordingly, *Itga5* and *Itgb1* were expressed at levels higher than *Pirb* in mouse epiphyseal cartilage [Fig. S6(A)], suggesting overall that α5β1 integrin serves as an ANGPTL2 receptor in chondrocytes.

Moreover, *Angptl2* knockdown markedly decreased p38 MAPK activation in ATDC5 cells relative to control shRNA cells [Fig. 6(B)]. Culture of those *Angptl2* knockdown cells with mouse rANGPTL2 increased p38 MAPK phosphorylation levels relative to control vehicle-treated *Angptl2* knockdown ATDC5 cells [Fig. 6(B)].

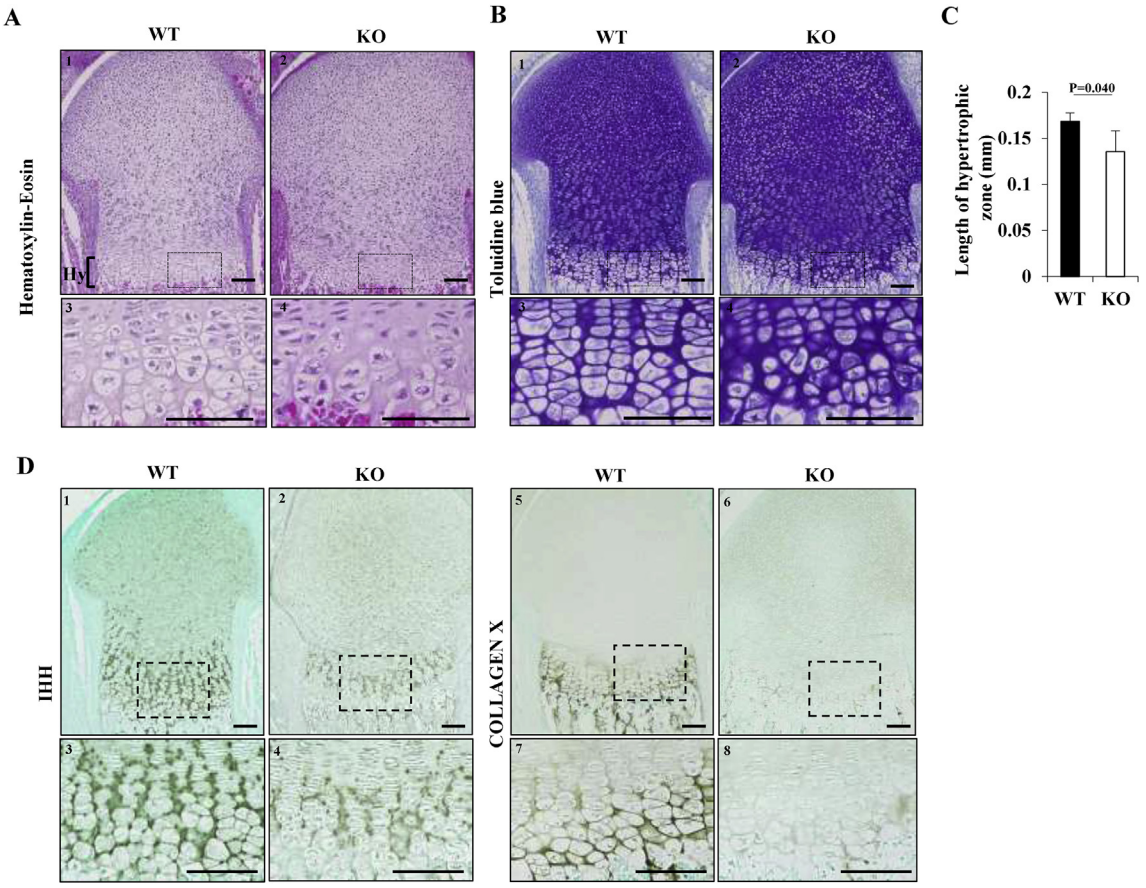


**Fig. 4. Cartilage of juvenile *Angptl2* knockout mice shows incomplete hypertrophic differentiation of chondrocytes**. (A) Representative images of hematoxylin and eosin staining, (B) toluidine blue staining and, (C) hypertrophic chondral zone length in wild-type and *Angptl2* knockout mice. ($n = 7$). (D) Immunohistochemistry with antibodies against IHH or COLLAGEN X in epiphyseal cartilage of newborn wild-type and *Angptl2* knockout mice. (A, B, and D) Panels 1, 3, 5, and 7, wild-type mice; panels 2, 4, 6, and 8, *Angptl2* knockout mice. Panels 3, 4, 7, and 8 are respective higher magnification images of hypertrophic zones (dashed squares) in 1, 2, 5, and 6. Hy: Hypertrophic zone. Scale bars (panels 1, 2, 5, and 6) = 100 μm. Scale bars (panels 3, 4, 7, and 8) = 50 μm. WT, wild-type mice; KO, *Angptl2* knockout mice. Results are expressed as means ± 95%CI. (C).

Interestingly, p38 MAPK activation induced by rANGPTL2 was not observed in ATDC5 cells treated with double *Angptl2*/*Itgb1* knockdown [Fig. 6(B)]. These data suggest that ANGPTL2 activates p38 MAPK phosphorylation through integrin α5β1 in ATDC5 cells.

Fourteen days after initiation of chondrogenic differentiation of ATDC5 cells by insulin, expression of transcripts encoding *Ihh*, a prehypertrophic chondrocyte marker, significantly increased compared to that seen in undifferentiated ATDC5 cells (data not shown). Expression of *Ihh* transcripts was significantly decreased in ATDC5 cells with stable knockdown of *Angptl2* relative to control shRNA cells [Fig. 6(C)]. rANGPTL2 treatment antagonized suppression of *Ihh* gene expression in *Angptl2* knockdown cells [Fig. 6(C)].

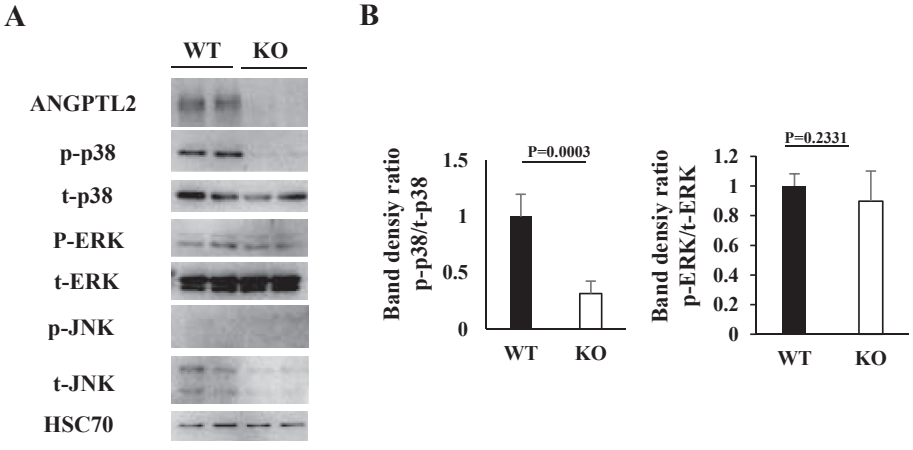


**Fig. 5. *In vivo* deletion of *Angptl2* decreases p38 activation in chondrocytes**. (A) Representative immunoblots showing ANGPTL2, phosphorylated p38 (p-p38), total p38 (t-p38), phosphorylated ERK1/2 (p-ERK), total ERK1/2 (t-ERK), JNK1/2 (p-JNK), total JNK1/2, and HSC70 in epiphyseal cartilage of newborn wild-type and *Angptl2* knockout mice. (B) Quantitative densitometry analysis of p-p38 and p-ERK immunoblots ($n = 5$). p-p38 values were normalized to t-p38, those of p-ERK to t-ERK. WT, wild-type mice; KO, *Angptl2* knockout mice. Wild-type values were set to 1, and densitometry values were expressed as fold increase relative to wild-type. Results are means as means ± 95%CI. (B).

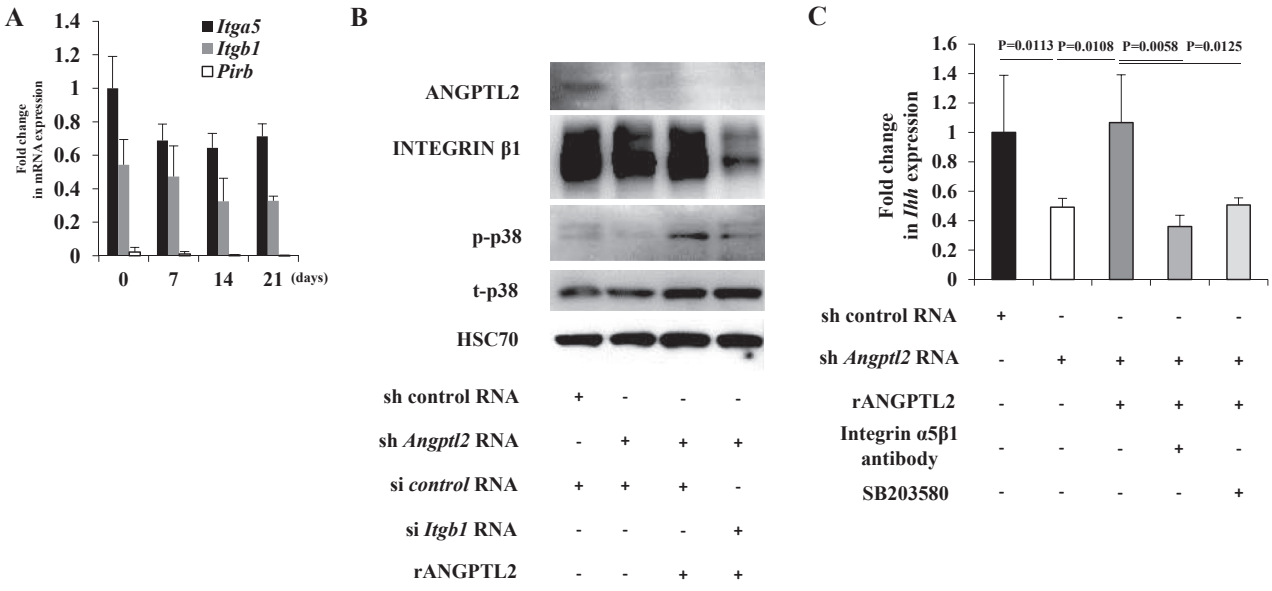


**Fig. 6. α5β1 Integrin is a candidate receptor for ANGPTL2 in chondrocytes**. (A) *Itga5*, *Itgb1* and *Pirb* transcript levels in ATDC5 cells at days 0, 7, 14, and 21 of chondrogenic cell differentiation. Transcript levels were normalized to *18s* ribosomal RNA and expressed as fold-increase relative to *Itga5* expression levels at day 0 ($n = 6$). (B) Representative images showing immunoblotting for ANGPTL2, Integrin β1, phosphorylated p38 (p-p38), total p38 (t-p38), and HSC70 in non-differentiated ATDC5 cells. Cells were harvested after 10 min of treatment with 5.0 μg/ml recombinant ANGPTL2 (rANGPTL2). (C) *Ihh* transcript levels in ATDC5 cells at day 14 post-differentiation. Integrin α5β1 antibody or SB203580 was added to cultures 60 min before stimulation with 5.0 μg/ml rANGPTL2. RNA was harvested 24 h after rANGPTL2 administration. Transcript levels were normalized to *18s* ribosomal RNA and expressed as fold-increase relative to control expression levels ($n = 4$). SB203580, p38 inhibitor. Results are expressed as means ± 95%CI (A, C).

However, further inhibition of integrin α5β1 with a neutralizing antibody against integrin α5β1 or inactivation of p38 MAPK with the p-38 inhibitor SB-203580 significantly suppressed *Ihh* induction [Fig. 6(C)]. Taken together, these data suggest that ANGPTL2 promotes chondrocyte differentiation by activating integrin α5β1 and p38 MAPK signaling.

### *Long bones in Angptl2 knockout mice are significantly shorter than those in control mice*

To assess whether ANGPTL2 functions in endochondral ossification during developmental bone growth, we compared bone length in *Angptl2* knockout relative to wild-type littermate mice. No gross skeletal abnormalities were seen in newborn *Angptl2* knockout mice (data not shown). However, microscopic evaluation revealed that long bone growth, as indicated by the ossified length of femurs or tibias, in *Angptl2* knockout mice was moderately but significantly reduced compared to wild-type mice [Fig. 7(A), (B)]. From 3 to 9 weeks after birth, *Angptl2* knockout mice showed continuous retardation of femur growth [Fig. 7(C)], a pattern also observed in long bones of 12-week-old *Angptl2* knockout relative to control mice [Fig. 7(D) and (E)].

### *SOX9-positive chondrocytes express abundant ANGPTL2 during repair-associated endochondral ossification*

Endochondral ossification is critical for fracture healing and bone regrowth[27]. Therefore, we asked whether ANGPTL2 is expressed in chondrocytes during bone repair after fracture. To do so, we performed a unilateral right side open transverse tibia osteotomy in wild-type adult mice, a procedure known as a bone fracture model with intramedullary needle fixation [Fig. 8(A)][28]. Real-time PCR analysis of bone tissue at the lesion in days after the osteotomy revealed that transcription of the chondrocyte marker *sox9* markedly increased and peaked by day 7 and then decreased from days 7–14 during the repair process [Fig. 8(B)]. Interestingly, *Angptl2* mRNA levels in fractured bone lesions also significantly increased in parallel with increased *sox9* transcript levels and decreased from days 7–14 [Fig. 8(B)]. Moreover, immunohistochemical analysis of serial sections of fractured bone on day 7 after osteotomy revealed ANGPTL2 expression in SOX9-positive chondrocytes and surrounding cartilaginous matrix in repairing bone [Fig. 8(C), panels 1–9]. These data suggest that ANGPTL2 may function in endochondral ossification not only during bone growth but in bone repair as well.

## Discussion

Our current study demonstrates that ANGPTL2 is expressed mainly in resting and proliferative chondrocytes, and that ANGPTL2 secreted by those chondrocytes accumulates in surrounding ECM. In *Angptl2* knockout mice, long bone growth was retarded from neonatal to adult stages due to differentiation of immature chondrocytes and was correlated with disruption in integrin α5β1 and p38 MAPK signaling during ossification. Our *in vitro* culture analysis reveals that ANGPTL2 promotes chondrocyte differentiation by activating α5β1 integrin and p38 signaling. Thus, ANGPTL2 functions in chondrocyte differentiation and subsequent endochondral ossification.

Integrin receptors reportedly play crucial roles in mediating signaling governing chondrocyte differentiation and endochondral ossification[5]. ANGPTL2 is characterized structurally by a C-terminal fibrinogen-like domain[11] reportedly important for binding with α5β1 integrin, a known fibronectin receptor in chondrocytes[12]. We previously reported that α5β1 integrin plays a critical role in ANGPTL2 function in several tissues[11–13], analyses that did not include chondrocytes. A previous report by others indicated anomalous chondrocyte differentiation and endochondral ossification in long bones of mice in which α5β1 integrin signaling had been blocked, phenotypes similar to those reported here in *Angptl2* knockout mice[29,30].

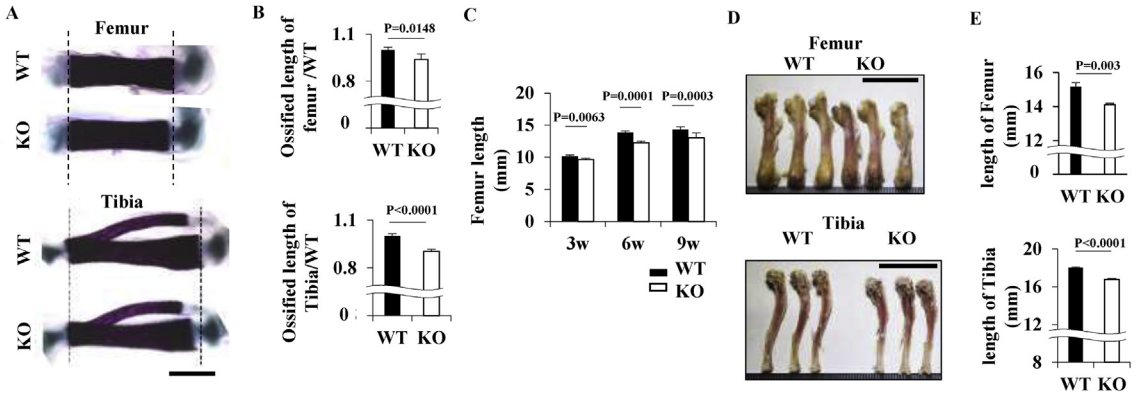


**Fig. 7. *Angptl2* deficiency retards long bone growth**. (A) Representative images of newborn mouse femurs (upper) and tibiae (lower) stained with Alizarin red and Alcian blue. Scale bars: 1 mm. (B) Ossified length of mice femurs (upper) and tibiae (lower) from wild-type or *Angptl2* knockout mice. Values are expressed as fold-increase relative to littermate wild-type mice ($n = 6$). (C) Femur length at 3, 6, and 9 weeks of age in wild-type and *Angptl2* knockout mice ($n = 3$–4 mice per group). (D) Upper panel: representative femurs from wild-type and *Angptl2* knockout mice at 12 weeks of age ($n = 3$). Lower panel: representative tibiae from wild-type and *Angptl2* knockout mice at 12 weeks of age. Scale bars: 10 mm. (E) femoral (upper) and tibial (lower) length in wild-type and *Angptl2* knockout mice at 12 weeks of age ($n = 4$ mice per group). Bone length is indicated in mm. WT, wild-type mice; KO, *Angptl2* knockout mice. Results are expressed as means ± 95%CI (B, C, and E).

In addition, p38 MAPK signaling is part of a major pathway governing bone development and remodeling[9,10]. For example, p38α ablation in differentiated chondrocytes suppresses their differentiation[31]; conversely, increased p38 phosphorylation drives chondrogenic differentiation and subsequent bone growth[32]. Our findings that ANGPTL2 likely regulates long bone growth through integrin/p38 MAPK signaling in chondrocytes is consistent with previous reports.

Structurally, ANGPTL2 is marked by an N-terminal coiled-coil domain (CCD)[11]. Some cartilage matrix component proteins that possess a CCD play important roles in maintaining cartilage homeostasis[4]. Recently, ANGPTL4, a different ANGPTL protein, was reported to function as an ECM protein that inhibits cell-adhesion, motility and tubule formation in endothelial cells[33]. Interestingly, that report showed that the ANGPTL4 CCD is critical for interaction with other ECM proteins such as heparin and dermatan sulfate chains[33] and that binding to other ECM proteins protects ANGPTL4 from proteolysis and preserves its bioactivity[33]. Our previous *in vitro* culture analysis of osteosarcoma cells showed that ANGPTL2 was inactivated by proteolytic cleavage[14]. Taken together with

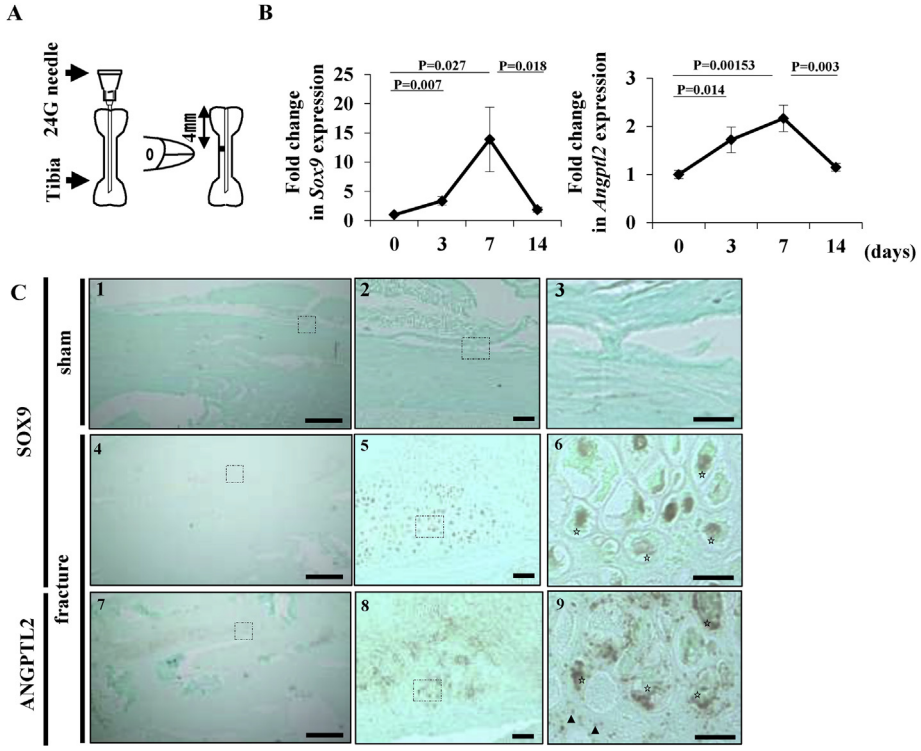


**Fig. 8. ANGPTL2 is expressed in callus cartilage after bone fracture**. (A) Schematic representation of the tibia osteotomy model. A 24-gauge needle was inserted into the long axis of mouse tibias. Osteotomy was performed 4 mm from tibial epiphysis (see Methods). (B) Graph showing *Sox9* (left) and (right) *Angptl2* (right) transcript levels in tibial tissue at days 0, 3, 7, and 14 after osteotomy in wild-type mice. Transcript levels were normalized to *18s* ribosomal RNA and expressed as fold-increase relative to day 0 ($n = 4$). (C) Panels 1–3, representative images of SOX9 immunostaining in sham-operated tibia. Panels 4–6 show similar SOX9 staining in fracture callus of osteotomy-treated tibia 7 days after osteotomy. Panels 7–9 show ANGPTL2 staining in a section adjacent to that shown in panels 4–6. Panels 2, 5 and 8 are respective higher magnification images of dashed squares in 1, 4 and 7; panels 3, 6 and 9 correspond to dashed squares in 2, 5 and 8. Stars indicate cells positive for both SOX9 and ANGPTL2. Arrowheads indicate ANGPTL2 accumulated in ECM. Scale bars (panels 1, 4, and 7) = 1 mm. Scale bars (panels 2, 5, and 8) = 100 μm. Scale bars (panels 3, 6, and 9) = 25 μm. Results are expressed as means ± 95%CI (B).

these findings, we conclude that the ANGPTL2 CCD may be important for retaining bioactivity by oligomer formation or by binding other ECM proteins to prevent proteolysis during chondrocyte differentiation and endochondral ossification. Further investigation of these mechanisms is required.

In addition to its relevance to physiological bone growth, endochondral ossification is important for bone fracture repair[34]. Interestingly, our mouse fracture model revealed that ANGPTL2 expression increases in callus chondrocytes during the repair process, suggesting that ANGPTL2 contributes to bone repair. Further investigation is needed to clarify how ANGPTL2 functions in this activity.

Retardation of long bone growth seen in *Angptl2* knockout mice was moderate rather than severe. In bone growth, complex signals between chondrocytes and extracellular factors likely fine-tune chondrocyte differentiation, and these signals may be redundant in regulating long bone growth[21]. Therefore, overlapping signals from different extracellular molecules may compensate for ANGPTL2 loss in *Angptl2* knockout mice. For example, *Angptl4* which is also accumulated in cartilage ECM is reportedly induced by hypoxia[35,36] and functions in cartilage remodeling by increasing *MMP* expression and decreasing expression of *Col2a1 or Acan*[37]. Here, we observed significantly decreased *Angptl4* transcript levels in *Angptl2* knockdown ATDC5 cells relative to controls by 21 days after the start of differentiation [Fig. S7(A)]. Furthermore, *in vivo* *Angptl4* expression in epiphyseal cartilage decreased in *Angptl2* knockout relative to wild-type mice [Fig. S7(B)]. These data suggest that in mice, *Angptl2* and *Angptl4* govern cartilage formation to some extent by regulating each other's expression. Although inside of epiphyseal cartilage tissue is hypoxic, the decrease in *Angptl4* expression seen following *Angptl2* loss may underlie the short limb phenotype of *Angptl2*-deficient mice. However, our current data suggests that ANGPTL2 regulates long bone growth in part by suppressing apoptosis or increasing cell proliferation through integrin α5β1/p38 MAPK-mediated IHH expression.

A limitation of this study is that it was not yet available to analyze using chondrocyte-specific *Angptl2* knockout mice, and we do not directly demonstrate that ANGPTL2 derived only from chondrocytes promotes endochondral ossification or fracture repair. Others have reported that ANGPTL2 is expressed in adipocytes, ligaments, macrophage, vascular endothelial cells or osteoblasts[11,13,38]. Therefore, we cannot rule out that ANGPTL2 derived from these cell types may regulate bone growth or fracture repair.

In conclusion, we have demonstrated that ANGPTL2 contributes to chondrocyte differentiation and subsequent endochondral ossification through the integrin α5β1/p38 MAPK signaling pathway to regulate bone growth. Our findings provide insight into molecular mechanisms governing communication between chondrocytes and surrounding ECM components in this process (Fig. S8).

## Author contributions

HT and JM designed the study and wrote the paper. HT, JM, TY, MY, HI, YU, TM, TN, HO, TS, TK, ME, KM, KT, and HO performed *in vitro* and *in vivo* experiments and provided technical assistance. ST, KY, TF, HM and YO provided critical supervision of the manuscript. All authors analyzed results and approved the final version of the manuscript.

## Conflict of interest

The authors declare that they have no conflicts of interest relevant to the content of this article.

## Acknowledgements

We thank Mss K. Tabu, M. Nakata and N. Shirai for technical assistance. This work was supported by the Core Research for Evolutional Science and Technology (CREST) program of Japan Agency for Medical Research and Development (AMED) (15gm0610007h0003).

## Supplementary data

Supplementary data related to this article can be found at https://doi.org/10.1016/j.joca.2017.10.011.

## References

1. Kronenberg HM. Developmental regulation of the growth plate. Nature 2003;423:332–6.
2. Schipani E, Ryan HE, Didrickson S, Kobayashi T, Knight M, Johnson RS. Hypoxia in cartilage: HIF-1alpha is essential for chondrocyte growth arrest and survival. Genes Dev 2001;15:2865–76.
3. Ateshian GA, Costa KD, Hung CT. A theoretical analysis of water transport through chondrocytes. Biomech Model Mechanobiol 2007;6:91–101.
4. Zaucke F, Grassel S. Genetic mouse models for the functional analysis of the perifibrillar components collagen IX, COMP and matrilin-3: implications for growth cartilage differentiation and endochondral ossification. Histol Histopathol 2009;24:1067–79.
5. Loeser RF. Integrins and cell signaling in chondrocytes. Biorheology 2002;39:119–24.
6. Gao Y, Liu S, Huang J, Guo W, Chen J, Zhang L, *et al*. The ECM-cell interaction of cartilage extracellular matrix on chondrocytes. Biomed Res Int 2014;2014648459.
7. Bobick BE, Kulyk WM. Regulation of cartilage formation and maturation by mitogen-activated protein kinase signaling. Birth Defects Res C Embryo Today 2008;84:131–54.
8. Beier F, Loeser RF. Biology and pathology of Rho GTPase, PI-3 kinase-Akt, and MAP kinase signaling pathways in chondrocytes. J Cell Biochem 2010;110:573–80.
9. Thouverey C, Caverzasio J. Focus on the p38 MAPK signaling pathway in bone development and maintenance. Bonekey Rep 2015;4:711.
10. Stanton LA, Sabari S, Sampaio AV, Underhill TM, Beier F. p38 MAP kinase signalling is required for hypertrophic chondrocyte differentiation. Biochem J 2004;378:53–62.
11. Kadomatsu T, Endo M, Miyata K, Oike Y. Diverse roles of ANGPTL2 in physiology and pathophysiology. Trends Endocrinol Metab 2014;25:245–54.
12. Tabata M, Kadomatsu T, Fukuhara S, Miyata K, Ito Y, Endo M, *et al*. Angiopoietin-like protein 2 promotes chronic adipose tissue inflammation and obesity-related systemic insulin resistance. Cell Metab 2009;10:178–88.
13. Nakamura T, Okada T, Endo M, Kadomatsu T, Taniwaki T, Sei A, *et al*. Angiopoietin-like protein 2 induced by mechanical stress accelerates degeneration and hypertrophy of the ligamentum flavum in lumbar spinal canal stenosis. PLoS One 2014;9:e85542.
14. Odagiri H, Kadomatsu T, Endo M, Masuda T, Morioka MS, Fukuhara S, *et al*. The secreted protein ANGPTL2 promotes metastasis of osteosarcoma cells through integrin alpha5-beta1, p38 MAPK, and matrix metalloproteinases. Sci Signal 2014;7:ra7.
15. Morinaga J, Kadomatsu T, Miyata K, Endo M, Terada K, Tian Z, *et al*. Angiopoietin-like protein 2 increases renal fibrosis by accelerating transforming growth factor-beta signaling in chronic kidney disease. Kidney Int 2016;89:327–41.
16. Shukunami C, Ishizeki K, Atsumi T, Ohta Y, Suzuki F, Hiraki Y. Cellular hypertrophy and calcification of embryonal

carcinoma-derived chondrogenic cell line ATDC5 in vitro. J Bone Min Res 1997;12:1174–88.
17. Shukunami C, Shigeno C, Atsumi T, Ishizeki K, Suzuki F, Hiraki Y. Chondrogenic differentiation of clonal mouse embryonic cell line ATDC5 in vitro: differentiation-dependent gene expression of parathyroid hormone (PTH)/PTH-related peptide receptor. J Cell Biol 1996;133:457–68.
18. Altaf FM, Hering TM, Kazmi NH, Yoo JU, Johnstone B. Ascorbate-enhanced chondrogenesis of ATDC5 cells. Eur Cell Mater 2006;12:64–9. discussion 69–70.
19. Morita S, Kojima T, Kitamura T. Plat-E: an efficient and stable system for transient packaging of retroviruses. Gene Ther 2000;7:1063–6.
20. Endo H, Murata K, Mukai M, Ishikawa O, Inoue M. Activation of insulin-like growth factor signaling induces apoptotic cell death under prolonged hypoxia by enhancing endoplasmic reticulum stress response. Cancer Res 2007;67:8095–103.
21. Posey KL, Hankenson K, Veerisetty AC, Bornstein P, Lawler J, Hecht JT. Skeletal abnormalities in mice lacking extracellular matrix proteins, thrombospondin-1, thrombospondin-3, thrombospondin-5, and type IX collagen. Am J Pathol 2008;172:1664–74.
22. Little C, Smith S, Ghosh P, Bellenger C. Histomorphological and immunohistochemical evaluation of joint changes in a model of osteoarthritis induced by lateral meniscectomy in sheep. J Rheumatol 1997;24:2199–209.
23. Tian F, Wu M, Deng L, Zhu G, Ma J, Gao B, *et al*. Core binding factor beta (Cbfbeta) controls the balance of chondrocyte proliferation and differentiation by upregulating Indian hedgehog (Ihh) expression and inhibiting parathyroid hormone-related protein receptor (PPR) expression in postnatal cartilage and bone formation. J Bone Min Res 2014;29:1564–74.
24. Motokawa I, Endo M, Terada K, Horiguchi H, Miyata K, Kadomatsu T, *et al*. Interstitial pneumonia induced by bleomycin treatment is exacerbated in Angptl2-deficient mice. Am J Physiol Lung Cell Mol Physiol 2016;311:L704–13.
25. Kato A, Fukuda T, Fukazawa Y, Isojima Y, Fujitani K, Inokuchi K, *et al*. Phorbol esters promote postsynaptic accumulation of Vesl-1S/Homer-1a protein. Eur J Neurosci 2001;13:1292–302.
26. Aoi J, Endo M, Kadomatsu T, Miyata K, Nakano M, Horiguchi H, *et al*. Angiopoietin-like protein 2 is an important facilitator of inflammatory carcinogenesis and metastasis. Cancer Res 2011;71:7502–12.
27. Vortkamp A, Pathi S, Peretti GM, Caruso EM, Zaleske DJ, Tabin CJ. Recapitulation of signals regulating embryonic bone formation during postnatal growth and in fracture repair. Mech Dev 1998;71:65–76.
28. Harry LE, Sandison A, Paleolog EM, Hansen U, Pearse MF, Nanchahal J. Comparison of the healing of open tibial fractures covered with either muscle or fasciocutaneous tissue in a murine model. J Orthop Res 2008;26:1238–44.
29. Inoue T, Hashimoto R, Matsumoto A, Jahan E, Rafiq AM, Udagawa J, *et al*. In vivo analysis of Arg-Gly-Asp sequence/integrin alpha5beta1-mediated signal involvement in embryonic enchondral ossification by exo utero development system. J Bone Min Res 2014;29:1554–63.
30. Garciadiego-Cazares D, Rosales C, Katoh M, Chimal-Monroy J. Coordination of chondrocyte differentiation and joint formation by alpha5beta1 integrin in the developing appendicular skeleton. Development 2004;131:4735–42.
31. Hutchison MR. Mice with a conditional deletion of the neurotrophin receptor TrkB are dwarfed, and are similar to mice with a MAPK14 deletion. PLoS One 2013;8:e66206.
32. Kim GW, Han MS, Park HR, Lee EJ, Jung YK, Usmani SE, *et al*. CXC chemokine ligand 12a enhances chondrocyte proliferation and maturation during endochondral bone formation. Osteoarthritis and Cartilage 2015;23:966–74.
33. Chomel C, Cazes A, Faye C, Bignon M, Gomez E, Ardidie-Robouant C, *et al*. Interaction of the coiled-coil domain with glycosaminoglycans protects angiopoietin-like 4 from proteolysis and regulates its antiangiogenic activity. FASEB J 2009;23:940–9.
34. Einhorn TA. The cell and molecular biology of fracture healing. Clin Orthop Relat Res 1998:S7–S21.
35. Knowles HJ. Multiple roles of angiopoietin-like 4 in osteolytic disease. Front Endocrinol (Lausanne) 2017;8:80.
36. Murata M, Yudo K, Nakamura H, Chiba J, Okamoto K, Suematsu N, *et al*. Hypoxia upregulates the expression of angiopoietin-like-4 in human articular chondrocytes: role of angiopoietin-like-4 in the expression of matrix metalloproteinases and cartilage degradation. J Orthop Res 2009;27:50–7.
37. Mathieu M, Iampietro M, Chuchana P, Guerit D, Djouad F, Noel D, *et al*. Involvement of angiopoietin-like 4 in matrix remodeling during chondrogenic differentiation of mesenchymal stem cells. J Biol Chem 2014;289:8402–12.
38. Takano A, Fukuda T, Shinjo T, Iwashita M, Matsuzaki E, Yamamichi K, *et al*. Angiopoietin-like protein 2 is a positive regulator of osteoblast differentiation. Metabolism 2017;69:157–70.